

Absence of Superconductivity in LK-99 at Ambient Conditions

Kapil Kumar, Navneet Kumar Karn, Yogesh Kumar, and V.P.S. Awana*

Cite This: *ACS Omega* 2023, 8, 41737–41743

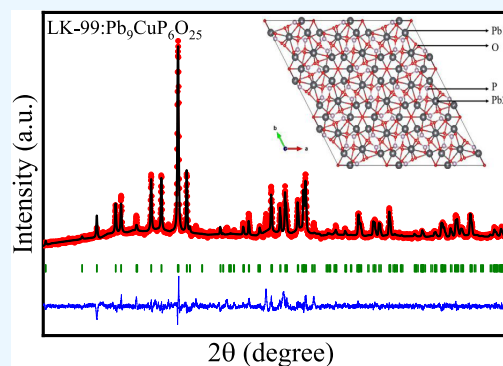
Read Online

ACCESS |

Metrics & More

Article Recommendations

ABSTRACT: The report of the synthesis of modified lead apatite (LK-99), with evidence of superconductivity at more than boiling water temperature, has steered the scientific community. There have been several failures to reproduce superconductivity in LK-99, despite partial successes. Here, we have continued our efforts to synthesize phase-pure LK-99 with improved precursors. The synthesis process being followed is the same as suggested by Sukbae Lee et al. The phase purity of each precursor is evidenced by powder X-ray diffraction (PXRD) and is well-fitted by Rietveld refinement. The PXRD confirms the synthesis of phase-pure polycrystalline LK-99 with a lead apatite structure. The sample is highly resistive, showing insulator-like behavior in resistivity measurement in the temperature range from 215 to 325 K, which confirms the absence of superconductivity in synthesized LK-99 at room temperature. The magnetization measurements of LK-99 on the SQUID magnetometer resemble the behavior of a resistive diamagnetic material at 280 K. Moreover, we have also performed first principle calculations to investigate the electronic band structure of LK-99 in the vicinity of the Fermi level. Our study verifies that the copper (Cu)-doped lead apatite (LK-99) exhibits band crossing at the Fermi level, indicating the generation of strong correlation in the presently studied system. Our experimental results do not approve the appearance of superconductivity in LK-99, i.e., $\text{Pb}_9\text{CuP}_6\text{O}_{25}$.



INTRODUCTION

The scientific community around the world is trying to reproduce the astonishing results of LK-99 (superconductivity near 400 K) shown by the Korean group.^{1–3} There have been two experimental reports^{4,5} showing negative primary evidence, including that of ours.⁵ A partial success in attaining superconductivity in the Cu-doped lead apatite is shown by Hou et al.⁶ However, they showed⁶ superconductivity below 110 K, which is way below the claimed superconductor transition temperature (T_c) of 400 K. Another recent report shows magnetic levitation of LK-99 at room temperature with a diamagnetic transition around 325 K.⁷ A close look at all attempts suggests that the phase purity of each precursor is crucial for the synthesis of LK-99, and this must be ensured before superconductivity is expected in the sample. Two mechanisms for superconductivity in LK-99 have been proposed by the original creators of LK-99: one is superconducting quantum well and the second is strong correlation due to enhanced Coulombic interaction by doping of copper.^{1,2} A quite good BR-BCS theory has been developed to predict the transition temperature T_c of high-temperature superconductors⁸ via a strong electron correlation mechanism. Recently, Baskaran^{9,10} has proposed an alternate mechanism, which suggests that there is a transition from a broadband Mott insulator to the superconducting region by introducing doping of the Cu atom in the lead apatite structure.⁹ These two mechanisms^{8,9} have opened up a new unbound number of

possible candidates of hot superconductors to be tried out experimentally. Other computational studies^{11–14} show that the parent lead apatite is a band gap insulator, but the doping of the Cu atom shows two isolated flat bands near the Fermi level. Interestingly, Liu et al.¹⁵ show that the substitution of Cu at different sites of Pb leads to distinct phases of LK-99, showing different electronic transport behavior. On the other hand, the two-band Hubbard model on a triangular lattice developed by Oh et al.¹⁶ suggests s-wave pairing. They show that LK-99 can be a possible low-temperature superconductor, when the obtained DFT parameters for the two-band model are clubbed with the Hubbard model.¹⁶ Interestingly, another first principle-based study¹⁷ envisages that Cu doping in LK-99 leads to ultraflat bands crossing the Fermi level due to hybridization of the Cu(3d) and O(2p) orbitals and possible superconductivity. Based on symmetry arguments, it is also envisaged¹⁸ that Cu-doped LK-99 may lead to possible ferroic properties. Interestingly, most of the results cited above are on cond-mat arxiv and have yet not been through the rigorous

Received: August 17, 2023

Accepted: October 4, 2023

Published: October 25, 2023



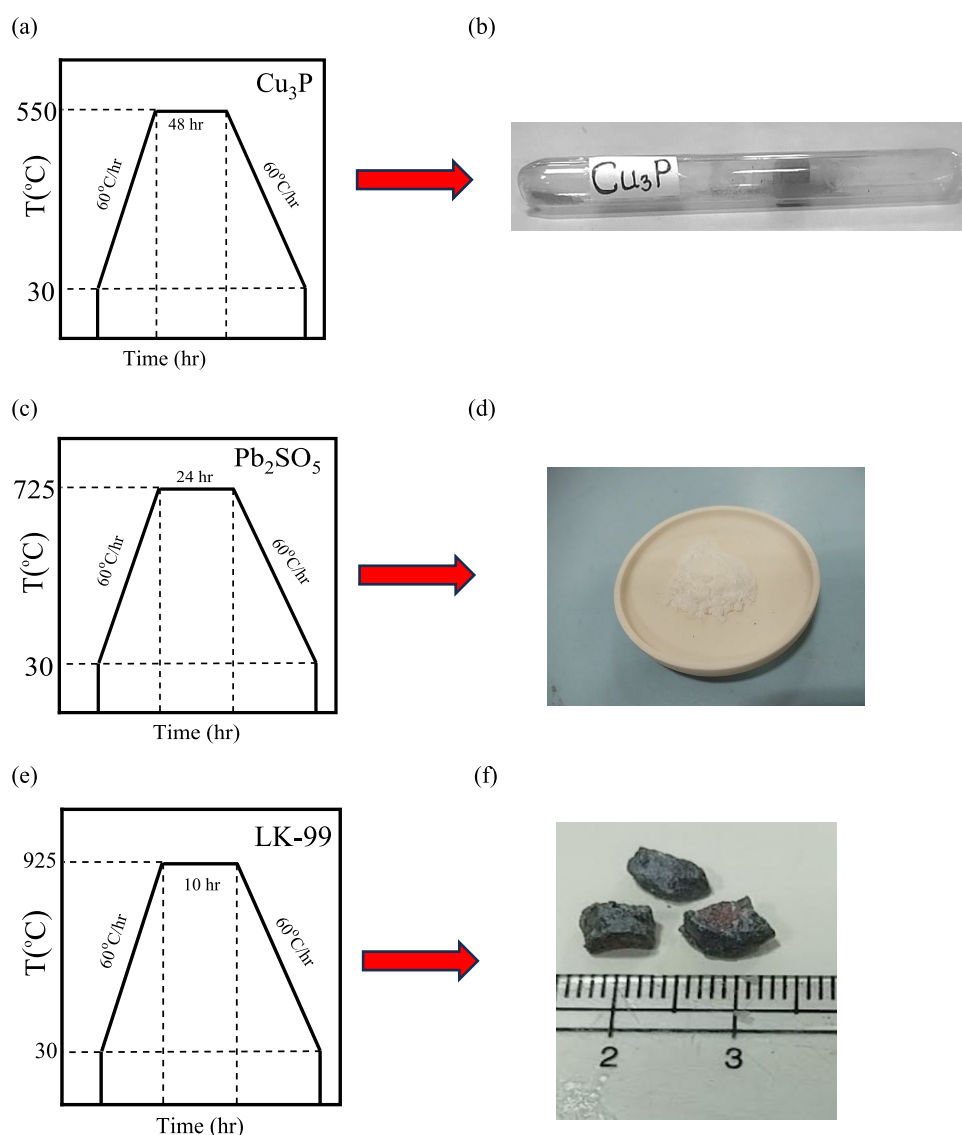


Figure 1. (a) Heat treatment diagram for Cu_3P (b) obtained product after heat treatment in a sealed quartz tube. (c) Heat treatment diagram for Pb_2SO_5 (d) delivered product after heat treatment in an open alumina crucible. (e) Heat treatment diagram for LK-99 synthesis and (f) small chunks of obtained polycrystalline sample.

peer review of SCI journals. This is because room-temperature superconductivity has been evolving fast since its inception.^{1,2}

This is our second attempt to find superconductivity in LK-99 as claimed by Lee et al.^{1,2} This time we used high-purity precursors. The same is evidenced by the synthesis of Cu_3P , where unreacted copper peaks are not found. In our previous report⁵ as well as in the partial success report,⁶ the PXRD of Cu_3P showed the unreacted peaks of Cu. However, this time there is no extra peak observed in the PXRD of Cu_3P . The phase purity of the synthesized LK-99 sample is confirmed by X-ray diffraction (XRD) measurement. In a most recent report,¹⁹ although the unreacted phase is visibly smaller than all earlier reports,^{1–6} it seems more than that of our present sample. To date, our sample seems to be the purest one in terms of phase purity. This is discussed in the Results section. Our results support the synthesis protocols as reported in ref 1,2 for phase-pure LK-99. For the robust test of superconductivity in LK-99, an electronic transport (resistivity) measurement and magnetic measurement are performed. The four-probe resistivity measurement confirms the absence of

superconductivity in LK-99 at room temperature, as the sample at room temperature is highly resistive, behaving like an insulator. The magnetization measurement also indicates the absence of superconductivity in modified lead apatite at room temperature. Our first principal studies support the mechanisms proposed by Kim,⁸ i.e., doping of Cu atoms at the Pb site enhances the electronic correlations in LK-99.

EXPERIMENTAL AND COMPUTATIONAL DETAILS

For the synthesis of the target sample of LK-99, the same protocol of refs 1,2,5, has been followed. The brief procedure is as follows: To synthesize the first precursor Cu_3P , a freshly bought brown chunk of phosphorus (P) from Sigma-Aldrich is ground with copper (Cu) powder in an argon-filled M-Braun glovebox. Exposure to an open atmosphere is strictly avoided. The ground powder is pelletized and vacuum sealed at 10^{-5} Torr and heated for 48 h at 550 $^{\circ}\text{C}$, as shown in Figure 1a. The resultant product encapsulated in a quartz ampule after heat treatment is shown in Figure 1b. The Cu powder from Merck is prechecked by PXRD to ensure the absence of CuO .

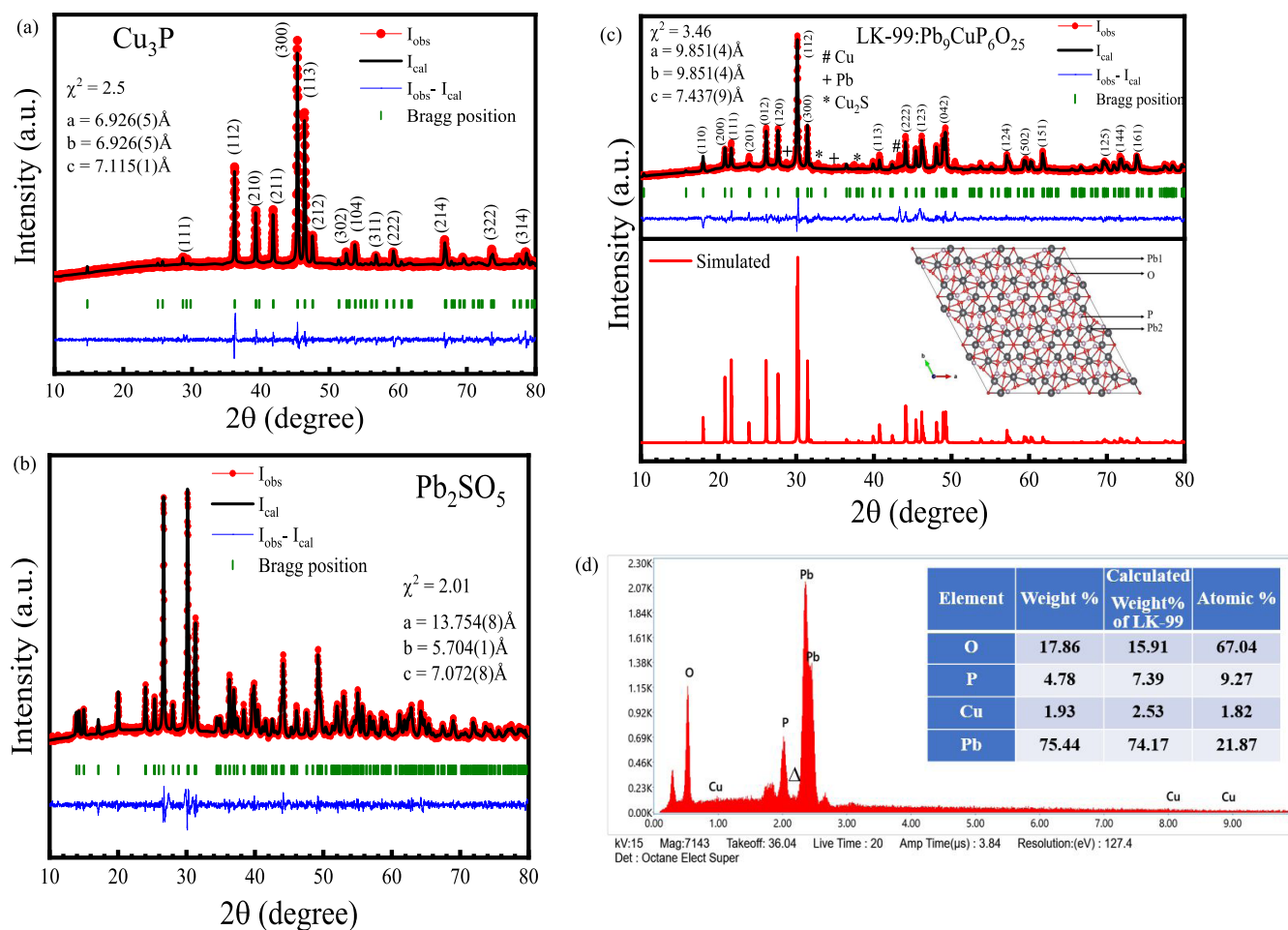
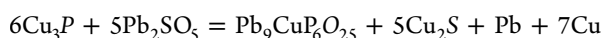


Figure 2. Rietveld refined PXRD pattern of the synthesized polycrystalline (a) Cu_3P , (b) Pb_2SO_5 , and (c) LK-99 and the bottom of (c) shows the simulated XRD pattern for apatite structure. The inset shows the top view of the apatite crystal structure. (d) EDX of the stoichiometry of constituent elements of LK-99, and the table in the inset shows the quantitative weight percentage and atomic percentage of all elements present in the sample.

Further, PbSO_4 and PbO being the essential elements for the production of other precursor Lanarkite Pb_2SO_5 are reacted. The chemical reaction that produces PbSO_4 is as follows: $\text{Pb}(\text{NO}_3)_2 + \text{H}_2\text{SO}_4 = \text{PbSO}_4 + 2\text{HNO}_3$.

The resultant, white color powder is dried in an oven, and its phase purity is validated using PXRD.⁵ To synthesize Lanarkite, the freshly prepared PbSO_4 is mixed with high-purity PbO (Sigma-Aldrich) and the mixture is put in an alumina crucible. The alumina crucible is subject to heat treatment as shown in Figure 1c, in which the sample is heated to 725 °C and annealed for 24 h.

After cooling down to room temperature, the white color Lanarkite is achieved, which is shown in Figure 1d. Using these two precursors, i.e., Cu_3P and Pb_2SO_5 mixed thoroughly in a 6:5 stoichiometric ratio, the palletized sample of LK-99 is vacuum sealed in the quartz tube and heated for 10 h at 925 °C as shown in Figure 1e. After heat treatment, the small polycrystalline chunks of the final product LK-99 are obtained, which are shown in Figure 1f. A possible chemical reaction leading to LK-99 synthesis is



During the whole synthesis process, the XRD spectra of all finely crushed powders of precursors were performed and the results were compared to the JCPDS data. The PXRD

measurements were performed by a Rigaku-Miniflex-II tabletop XRD equipped with $\text{Cu K}\alpha$ radiation of 1.54 Å. FullProf software is used to perform the Rietveld refinement of the obtained PXRD spectra. The elemental compositions were examined by performing an energy-dispersive X-ray spectroscopy (EDX) measurement using a Zeiss EVO-50 instrument. For a robust test of superconductivity, the conventional four-probe arrangement is used to measure the electrical transport properties of the synthesized crystals. This method is employed in conjunction with a 14 T Cryogenic Physical Property Measurement System (PPMS). The magnetization measurement was performed on the SQUID magnetometer at 280 K.

To determine the correlation effects induced due to Cu doping in lead oxyapatite, we have performed first principle calculations. For this, we use first principle methods based on the density functional theory implemented in QUANTUM ESPRESSO to obtain the electronic band structure and density of states (DOS) of doped LK-99. A system of 41 atoms is simulated on a $4 \times 4 \times 5$ grid of Monkhorst-Pack. The Perdew–Burke–Ernzerhof (PBE)-type ultrasoft pseudopotential with a generalized gradient approximation (GGA) is used to account for the electronic exchange and correlation. The wave functions are expanded in a plane wave basis with Gaussian smearing of the width 0.01. For the convergence of

Table 1. Parameters Obtained from the Rietveld Refinement

	<i>a</i> (Å)	<i>b</i> (Å)	<i>c</i> (Å)	α (deg)	β (deg)	γ (deg)	χ^2
Cu ₃ P	6.926(5)	6.926(5)	7.115(1)	90	90	120	2.5
Pb ₂ SO ₅	13.754(8)	5.704(1)	7.072(8)	90	115	90	2.01
LK-99	9.851(4)	9.851(4)	7.437(9)	90	90	120	3.46

self-consistent calculation, the cutoff is 8.8×10^{-9} Ry, a charge cutoff of 400 Ry, and a wave function cutoff of 50 Ry is used.

RESULTS AND DISCUSSION

Figure 2a shows the Rietveld refined data of the recorded PXRD spectra of Cu₃P by using FullProf software. The red and black curves represent the experimentally observed and calculated intensity, respectively, whereas the blue curve shows the difference between the two. The Bragg's positions are represented by vertical green bars. The refinement is well fitted in the hexagonal phase with space group P63 cm (185). The agreement of calculated intensity by Rietveld refinement with the observed data confirms the absence of any impurity in the synthesized material. The obtained lattice parameters are $a = b = 6.926(5)$ Å and $c = 7.115(1)$ Å. The quality of fit in the Rietveld refinement is assessed using the parameter χ^2 , which has a value of 2.5; a lower χ^2 value indicates a better fit between the experimental data and the calculated data. Importantly, the Rietveld refinement analysis clearly shows that the synthesized Cu₃P does not contain any extra peak of unreacted copper. This observation is in contrast to our previous report,⁵ where we had observed the presence of unreacted copper peaks in the PXRD pattern. This time, we used a fresh chunk of phosphorus and Cu, also Cu was prechecked for any CuO contamination. The absence of unreacted copper peaks suggests that the synthesis of Cu₃P has been successful and complete, without any significant leftover from the starting materials. This indicates the completion of the desired reaction and the formation of the target material. Figure 2b shows the Rietveld refined data of recorded PXRD spectra of Lanarkite (Pb₂SO₅) by using FullProf software. The Rietveld refinement of the PXRD data is fitted with a monoclinic lattice, which belongs to the P21/m space group and the obtained lattice parameters are $a = 13.754(8)$ Å, $b = 5.7046(1)$ Å, and $c = 7.072(8)$ Å. Through Rietveld refinement, it is observed that both the calculated and observed data points resemble each other, which suggests the purity of the as-synthesized Pb₂SO₅. The goodness of fit (χ^2) value is 2.01, which also indicates the phase purity of our material and the absence of any other phase.

After confirming the formation of the as-synthesized Cu₃P and Pb₂SO₅, both were taken in a stoichiometric ratio of 6:5 and vacuum sealed in a quartz ampule. After the heat treatment protocol is followed (Figure 1(e)), the polycrystalline sample of LK-99 is obtained. This sample is named LK-99. The PXRD of the as-obtained polycrystalline LK-99 samples is shown in Figure 2c. A few small peaks are observed as well, which may belong to the byproduct of synthesized LK-99. It is worth noting that the level of foreign phases, in particular Cu₂S, is relatively much smaller than the reported ones.^{1,2,4,5,19} The goodness of Rietveld fitting, i.e., (χ^2) value is 3.46, which is reasonable. In the bottom of Figure 2c, the simulated XRD pattern of the apatite structure is shown, and the inset shows the top view of the apatite structure. All major peaks of LK-99 match with the simulated XRD of the apatite structure. The Rietveld refinement of the PXRD data of LK-99 is well fitted in

the hexagonal phase with the space group P63/m (176) and the calculated lattice parameters of LK-99 are $a = b = 9.851(4)$ Å and $c = 7.437(9)$ Å. There is a slight shrinkage as compared to that of the lead apatite structure, which indicates the substitution of copper atoms to the atomic sites of lead atoms.¹ The lattice parameters for the pure lead apatite are known²⁰ to be $a = b = 9.865(3)$ Å and $c = 7.431(3)$ Å. There is a slight reduction of 0.18% in volume, which is in accordance with the contraction of unit cell parameters due to the Pb site Cu substitution. The small intensity of the byproduct peaks of Cu (#), Cu₂S (*), and Pb (+) are marked in PXRD of presently studied LK-99 in Figure 2c. All of the refined lattice parameters for used precursors (Cu₃P, Pb₂SO₅) and resultant LK-99 are shown in Table 1. From the XRD refinement of the present LK-99, it can be concluded that the same is almost pure phase. Further, the elemental composition of polycrystalline LK-99 is studied by performing EDX measurements. Figure 2d shows the observed EDX spectra; the observed peaks show the presence of all constituent elements of LK-99. Some unidentified peaks are also observed, which suggests the presence of minimal impurity. The table in the inset shows the quantitative weight percentage and atomic percentage of all elements present in the sample within the experimental limits. We also noticed that in elemental analysis, sulfur peaks were too minimal to be autodetected. The K_{α} energy for a sulfur atom is 2.307 eV, and the same peak in EDX spectra is marked by (Δ), which is very small showing a tiny amount of sulfur present. The Cu peaks are observed, indicating the presence of Cu in the sample matrix. Thus, the peaks of sulfur and Cu in EDX spectra confirm the presence of a small amount of Cu₂S phase, as also indicated by the XRD analysis. The quantitative weight percent confirms the nearly stoichiometric elemental composition of LK-99 within the EDX measurement uncertainty limit, which is quite high ($\sim 14.49\%$). Uncertainty is so large that the exact atomic weights cannot be reliably determined. However, all constituent elements are found to be near the nominal composition, and the observed stoichiometry of the synthesized sample is Pb₉Cu_{0.76}P_{3.82}O_{27.6}. Further characterization is required to investigate the exact substitution of Cu atoms on Pb(+2) atomic sites, say, by synchrotron radiation. Within XRD and EDX limits, one can safely conclude that the studied LK-99 is near phase pure, with a slight reduction in its volume in comparison to that of lead apatite, indicating possible Cu substitution at the Pb site. Till now, the storyline seems to be as good as being reported^{1,2} for superconducting LK-99.

Next, we examine the acquired LK-99's superconducting characteristics. The primary characteristic of a superconductor is vanishing resistance below the critical temperature. Figure 3 shows the electrical transport measurements of the synthesized polycrystalline LK-99 in the temperature range 215–325 K. The resistivity vs temperature (ρ -T) plot shows that the resistivity increases as the temperature decreases. The measured value of resistivity at 325 K is 25.2 Ω -m, which increases to 2.3×10^5 Ω -m at 215 K. This clearly shows a band gap insulator behavior. The (ρ -T) plot also asserts the

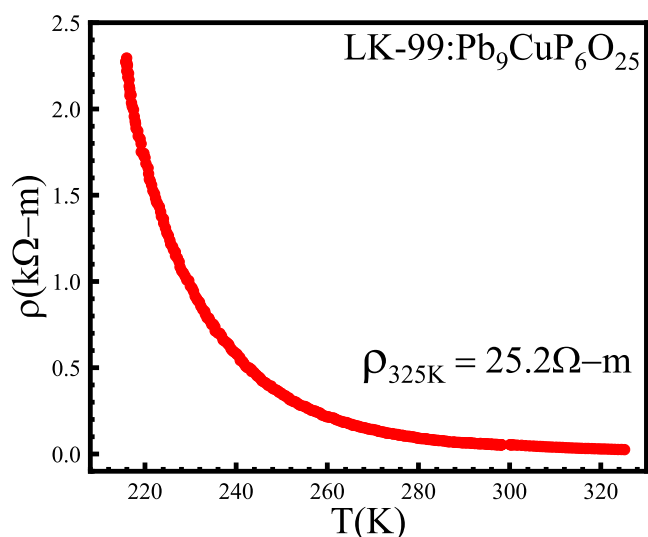


Figure 3. Temperature dependence of resistivity of synthesized LK-99.

absence of room-temperature superconductivity in the synthesized LK-99 as resistivity has the order of $\sim 10^2 \Omega\text{-m}$ at room temperature.

Further, the magnetic properties are studied by performing the isothermal magnetization (MH) measurements at 280 K by using a SQUID magnetometer. Figure 4a shows the linear dependence of magnetization on the applied field with a negative slope. Figure 4b shows the magnetization variation

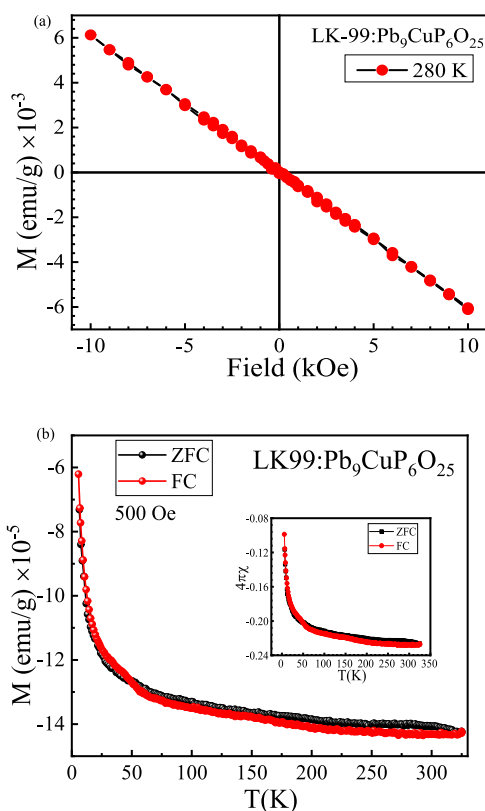


Figure 4. (a) Isothermal magnetization (MH) of the synthesized LK-99 samples at 280 K. (b) M - T curve for 500 Oe revealing diamagnetism in LK-99 and the inset figure shows the calculated magnetic susceptibility from M - T measurement.

with respect to temperature (M - T profile) for our synthesized LK-99 with Field Cool (FC) and Zero Field Cool (ZFC) protocols. The M - H curve at 280 K and M - T curve at 500 Oe for LK-99 are similar to those of NbAs_2 , which is a diamagnetic material,²¹ and the similar behavior in the M - T profile of recently synthesized single crystals of LK-99 by Puphal et al.²² The linear diamagnetic hysteresis in the M - H plot is also observed in superconducting Pb wires,²³ which is expected for a perfect superconducting sample with no pinning centers and without demagnetization corrections in magnetization loop. However, here the linear loop is very unlikely to be attributable to the presence of a superconducting phase, as LK-99 is highly resistive and polycrystalline with some minor impurities. A Curie-like upturn is observed in the M - T plot, with no superconducting anomaly seen in the temperature range of 5–325 K. The inset of Figure 4b shows the calculated mass magnetic susceptibility. At 315 K, the magnetic susceptibility is -0.23 , which increases to -0.098 at 5 K, resembling the behavior of an insulator. For superconductors, below T_c , usually magnetic susceptibility decreases as temperature decreases. Thus, the magnetic susceptibility curve with respect to the temperature of our LK-99 exhibits a diamagnetic behavior but not that of a superconductor. Also, our results are in accordance with a very recent report by Zhu et al., who claim that this behavior is possibly due to the first-order phase transition of Cu_2S from the β -phase to γ -phase in the present material.²⁴ Thus, magnetization measurement shows that although the current sample exhibits diamagnetic behavior, it does not support the presence of superconductivity as the magnetization starts increasing as the temperature decreases, like a resistive diamagnetic material. In conclusion, Figures 3 and 4 show that we have not yet been able to substantiate the assertions made in ref 1,2 about the superconductivity of LK-99 at ambient temperature. As far as magnetic properties of LK-99 are concerned, superconductivity above 400 K,^{1,2} paramagnetism at 280 K,⁵ ferroic nature,¹⁸ and simple diamagnetism in our present sample are reported. In terms of phase purity, the presently studied LK-99 seems to be better than the earlier reported ones.^{1,2,5,6,19} Although the contraction in cell volume of the presently studied LK-99 indicates the substitution of Cu at the Pb site in the lead apatite structure, the superconductivity is not observed.

Figure 5a shows the calculated DOS plot of lead apatite and LK-99. A finite value of DOS shows that the doping of Cu introduces a bulk conduction channel in LK-99. However, the parent compound lead apatite is insulating. Figure 5b shows the optimized path chosen for the electronic band structure calculation in the hexagonal first Brillouin zone. Figure 5c,d shows the calculated band structure in the first Brillouin zone of lead apatite and LK-99 along the highly symmetric path Γ - M - K - Γ - A - L - H - A . The bulk electronic band structure of lead apatite clearly shows that it is an insulator. However, the electronic band structure of LK-99 shows that there are bands close to the Fermi level crossing the same as shown in Figure 5e. This indicates the possible transition of LK-99 from an insulator to a conductor. It is clear that correlation effects are enhanced due to the doping of Cu. In ref, 15, computationally two phases, 6h (conducting) and 4f (insulating) of LK-99, are predicted based on the Cu substitution of the Pb site. Our computational result matches with the 6h phase of $\text{Pb}_9\text{CuP}_6\text{O}_{25}$, which is conducting. Following our experimental results, which show the insulating behavior of LK-99, it is quite possible that in our sample, the Cu substitution took place to

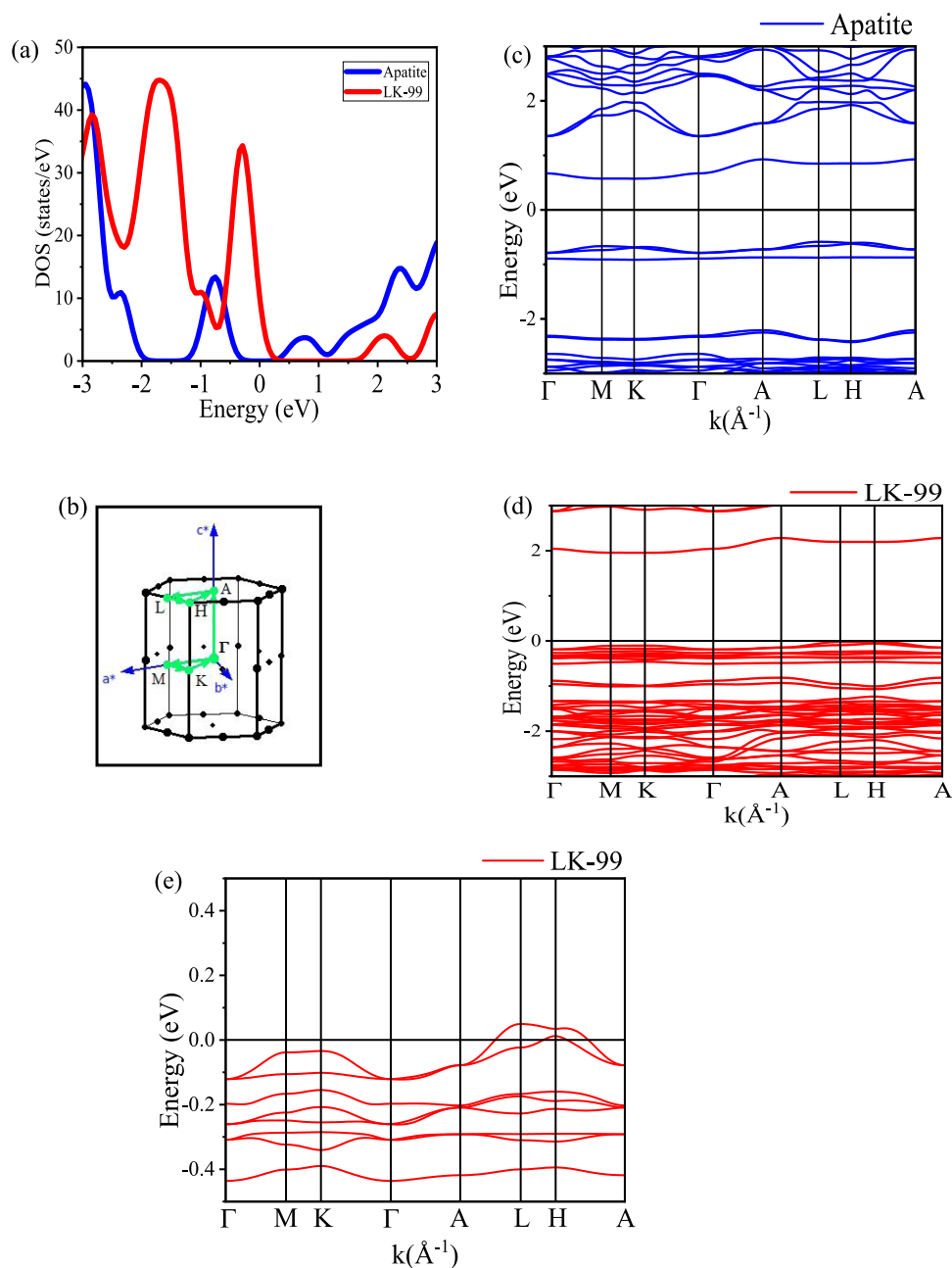


Figure 5. (a) Shows the DOS of apatite and LK-99. (b) k -path along which electronic bands are calculated. (c) Electronic band structure of lead apatite. (d) Calculated bulk electronic band structure of LK-99, where bands are crossing the Fermi Level. (e) Enlarged view of bands near the Fermi level.

form the 4f phase of LK-99. Therefore, we identify that our synthesized sample of LK-99 has a 4f phase based on experimental results. The single crystal synthesized by Puphal et al.²² has an inhomogeneous Cu substitution to the Pb site, which is not the exact 6h phase of computationally predicted conducting LK-99. Thus, for experimentalists, the open challenge remains to precisely synthesize the 6h phase of LK-99 reported in ref 15.

CONCLUSIONS

Summarily, we synthesized phase-pure precursors of LK-99, as confirmed by the Rietveld analysis of the PXRD data. Further, we report the successful synthesis of LK-99, following the same method as suggested in ref 1,2. The PXRD data and its

Rietveld refinement of LK-99 show the shrinkage in lattice parameters, leading to a 0.18% volume contraction compared to the parent compound lead apatite. However, the intriguing superconductivity as claimed in ref 1,2 appears to be elusive. The $(\rho-T)$ plot asserts the absence of room-temperature superconductivity in synthesized LK-99. The isothermal magnetization measurements at 280 K and the $M-T$ measurement show that the prepared sample is diamagnetic, but without any signatures of superconductivity. The experimental results for the synthesized phase of LK-99 reveal no superconductivity in LK-99.

AUTHOR INFORMATION

Corresponding Author

V.P.S. Awana – CSIR-National Physical Laboratory, New Delhi 110012, India; Academy of Scientific and Innovative Research (AcSIR), Ghaziabad 201002, India; orcid.org/0000-0002-4908-8600; Phone: +91-11-45609357; Email: awana@nplindia.org; Fax: +91-11-45609310; awanavps.webs.com

Authors

Kapil Kumar – CSIR-National Physical Laboratory, New Delhi 110012, India; Academy of Scientific and Innovative Research (AcSIR), Ghaziabad 201002, India

Navneet Kumar Karn – CSIR-National Physical Laboratory, New Delhi 110012, India; Academy of Scientific and Innovative Research (AcSIR), Ghaziabad 201002, India; orcid.org/0000-0003-1095-1371

Yogesh Kumar – CSIR-National Physical Laboratory, New Delhi 110012, India; Academy of Scientific and Innovative Research (AcSIR), Ghaziabad 201002, India

Complete contact information is available at: <https://pubs.acs.org/10.1021/acsomega.3c06096>

Notes

The authors declare no competing financial interest.

ACKNOWLEDGMENTS

The authors would like to acknowledge the keen interest of Prof. Achanta Venu Gopal, Director CSIR-NPL in superconducting materials research. They are thankful to Dr. J.S. Tawale for SEM measurements and Dr. S. Patnaik for resistivity measurement on PPMS. Dr. Pallavi Kushwaha is acknowledged for providing the SQUID magnetometer-based magnetization measurements for our sample. The motivation and encouragement of Prof. G. Baskaran (IMSc/IITM) and Prof. D.D. Sarma (IISc) has been very instrumental in carrying out this research. V.P.S. Awana acknowledges various fruitful discussions with Prof. I. Felner from Hebrew University Jerusalem concerning the observation of possible superconductivity in LK-99. The research is supported by an in-house project OLP-230232.

REFERENCES

- (1) Lee, S.; Kim, J. H.; Kwon, Y. W. The First Room-Temperature Ambient-Pressure Superconductor. 2023, arXiv:2307.12008. arXiv.org e-Print archive. <https://arxiv.org/abs/2307.12008>.
- (2) Lee, S.; Kim, J.; Kim, H. T.; Im, S.; An, S.; Auh, K. H. Superconductor $\text{Pb}_{10-x}\text{Cu}_x(\text{PO}_4)_6\text{O}$ showing levitation at room temperature and atmospheric pressure and mechanism. 2023, arXiv:2307.12037. arXiv.org e-Print archive. <https://arxiv.org/abs/2307.12037>.
- (3) Lee, S.; Kim, J.; Im, S.; An, S.; Kwon, Y. W.; Ho, A. K. Consideration for the development of room-temperature ambient-pressure superconductor (LK-99). *J. Korean Cryst. Growth Cryst. Technol.* **2023**, *33*, No. 61.
- (4) Liu, L.; Meng, Z.; Wang, X.; Chen, H.; Duan, Z.; Zhou, X.; Yan, H.; Qin, P.; Liu, Z. Semiconducting Transport in $\text{Pb}_{10-x}\text{Cu}_x(\text{PO}_4)_6\text{O}$ Sintered from Pb_2SO_5 and Cu_3P . *Adv. Funct. Mater.* **2023**, No. 2308938.
- (5) Kumar, K.; Karn, N. K.; Awana, V. P. S. Synthesis of possible room temperature superconductor LK-99: $\text{Pb}_9\text{Cu}(\text{PO}_4)_6\text{O}$. *Sup. Sci. Technol.* **2023**, *36*, No. 10LT02.
- (6) Hou, Q.; Wei, W.; Zhou, X.; Sun, Y.; Shi, Z. Observation of zero resistance above 100 K in $\text{Pb}_{10-x}\text{Cu}_x(\text{PO}_4)_6\text{O}$. 2023,

arXiv:2308.01192. arXiv.org e-Print archive. <https://arxiv.org/abs/2308.01192>.

(7) Wu, H.; Yang, L.; Xiao, B.; Chang, H. Successful growth and room temperature ambient-pressure magnetic levitation of LK-99. 2023, arXiv:2308.01516. arXiv.org e-Print archive. <https://arxiv.org/abs/2308.01516>.

(8) Kim, H. T. Room-temperature-superconducting Tc driven by electron correlation. *Sci. Rep.* **2021**, *11*, No. 10329.

(9) Baskaran, G. Broad Band Mott Localization is all you need for Hot Superconductivity: Atom Mott Insulator Theory for Cu-Pb Apatite. 2023, arXiv:2308.01307. arXiv.org e-Print archive. <https://arxiv.org/abs/2308.01307>.

(10) Baskaran, G. Impurity band Mott insulators: a new route to high Tc superconductivity. *Sci. Technol. Adv. Mater.* **2008**, *9*, No. 044104.

(11) Cabezas-Escases, J.; Barrera, N. F.; Cardenas, C.; Munoz, F. Theoretical insight on the LK-99 material. 2023, arXiv:2308.01135. arXiv.org e-Print archive. <https://arxiv.org/abs/2308.01135>.

(12) Kurleto, R.; Lany, S.; Pashov, D.; Acharya, S.; van Schilfgaarde, M.; Dessau, D. S. Pb-Apatite framework as a generator of novel flat-band CuO based physics, including possible room temperature superconductivity. 2023, arXiv:2308.00698. arXiv.org e-Print archive. <https://arxiv.org/abs/2308.00698>.

(13) Si, L.; Held, K. Electronic structure of the putative room-temperature superconductor $\text{Pb}_9\text{Cu}(\text{PO}_4)_6\text{O}$. 2023, arXiv:2308.00676. arXiv.org e-Print archive. <https://arxiv.org/abs/2308.00676>.

(14) Lai, J.; Li, J.; Liu, P.; Sun, Y.; Chen, X. Q. First-principles study on the electronic structure of $\text{Pb}_{10-x}\text{Cu}_x(\text{PO}_4)_6\text{O}$ ($x = 0,1$). *J. Mater. Sci. Technol.* **2024**, *171*, 66.

(15) Liu, R.; Guo, T.; Lu, J.; Ren, J.; Ma, T. Different phase leads to different transport behavior in $\text{Pb}_{10-x}\text{Cu}_x(\text{PO}_4)_6\text{O}$ compounds. 2023, arXiv:2308.08454. arXiv.org e-Print archive. <https://arxiv.org/abs/2308.08454>.

(16) Oh, H.; Zhang, Y.-H. S-wave pairing in a two-orbital t-j model on triangular lattice: possible application to $\text{Pb}_{10-x}\text{Cu}_x(\text{PO}_4)_6\text{O}$. 2023, arXiv:2308.02469. arXiv.org e-Print archive. <https://arxiv.org/abs/2308.02469>.

(17) Tao, K.; Chen, R.; Yang, L.; Gao, J.; Xue, D.; Jia, C. The Cu induced ultraflat band in the room-temperature superconductor $\text{Pb}_{1-x}\text{Cu}_x(\text{PO}_4)_6\text{O}$ ($x = 0,0.5$). 2023, arXiv:2308.03218. arXiv.org e-Print archive. <https://arxiv.org/abs/2308.03218>.

(18) Hlinka, J. Possible Ferroic properties of Copper-substituted lead phosphate Apatite. 2023, arXiv:2308.03691. arXiv.org e-Print archive. <https://arxiv.org/abs/2308.03691>.

(19) Guo, K.; Li, Y.; Jia, S. Ferromagnetic half levitation of LK-99-Like synthetic samples. *Sci. China: Phys., Mech. Astron.* **2023**, *66*, No. 107411.

(20) Krivovichev, S. V.; Burns, P. C. Crystal chemistry of Lead Oxide Phosphates: Crystal Structures of $\text{Pb}_4\text{O}(\text{PO}_4)_2$, $\text{Pb}_4\text{O}_8(\text{PO}_4)_2$ and $\text{Pb}_{10}(\text{PO}_4)_6\text{O}$. *Z. Kristallogr.* **2003**, *218*, 357.

(21) Peramaiyan, G.; Sankar, R.; Muthuselvan, I. P.; Lee, W. L. Anisotropic magnetotransport and extremely large magnetoresistance in NbAs_2 single crystals. *Sci. Rep.* **2018**, *8*, No. 6414.

(22) Puphal, P.; Akbar, M. Y. P.; Hepting, M.; Goering, E.; Isobe, M.; Nugroho, A. A.; Keimer, B. Single crystal synthesis, structure, and magnetism of $\text{Pb}_{10-x}\text{Cu}_x(\text{PO}_4)_6\text{O}$. 2023, arXiv:2308.06256. arXiv.org e-Print archive. <https://arxiv.org/abs/2308.06256>.

(23) Hwang, S. M. et al. Superconductors in SQUID-based ultralow field NMR—Flux-trapping in type-II wires, *IEEE Transactions on Applied Superconductivity*, 2014; Vol. 25(3), pp. 1–4.

(24) Zhu, S.; Wu, W.; Li, Z.; Luo, J. First order transition in $\text{Pb}_{10-x}\text{Cu}_x(\text{PO}_4)_6\text{O}$ ($0.9 < x < 1.1$) containing Cu_2S . 2023, arXiv:2308.04353. arXiv.org e-Print archive. <https://arxiv.org/abs/2308.04353>.